Deviation from local thermodynamic equilibrium in a cesium-seeded argon plasma

THE
Research Report

Eindhoven
University of Technology
Netherlands

Department of Electrical Engineering

Deviation from Local Thermodynamic Equilibrium in a Cesium-Seeded Argon Plasma

By
B. Stefanov, L. Zarkova and A. Veefkind

EUT Report 85-E-152
ISBN 90-6144-152-8
ISSN 0167-9708

November 1985

Eindhoven University of Technology Research Reports

EINDHOVEN UNIVERSITY OF TECHNOLOGY

Department of Electrical Engineering

Eindhoven The Netherlands

DEVIATION FROM LOCAL THERMODYNAMIC EQUILIBRIUM IN A CESIUM-SEEDED ARGON PLASMA

by

B. Stefanov

L. Zarkova

A. Veefkind

EUT Report 85-E-152

ISBN 90-6144-152-8

ISSN 0167-9708

Coden: TEUEDE

Eindhoven

November 1985

CIP-GEGEVENS KONINKLIJKE BIBLIOTHEEK, DEN HAAG

Stefanov, B.

Deviation from local thermodynamic equilibrium in a cesium-seeded argon plasma / by B. Stefanov, L. Zarkova and A. Veefkind. - Eindhoven: University of Technology. - Fig., tab. - (Eindhoven University of Technology research reports / Department of Electrical Engineering, ISSN 0167-9708; 85-E-152)
Met lit. opg., reg.
SISO 535 UDC 537.5 UGI 590
Trefw.: plasmafysica / magnetohydrodynamica.

Contents

Deviation from local thermodynamic equilibrium in a cesium-seeded argon plasma

B. Stefanov and L. Zarkova

Institute of Electronics, Bd. Lenin 72, Sofia 1184, Bulgaria

A. Veefkind

Group Direct Energy Conversion, Eindhoven University of Technology,
P.O. Box 513, 5600 MB Eindhoven, The Netherlands

Abstract

The possibility of deviations from local thermodynamic equilibrium of a cesium seeded argon plasma has been analyzed. A four level model of cesium has been employed. Overpopulations of the ground state and the first excited state as well as the corresponding reduction of the electron density are calculated for cylindrical discharge structures by solving stationary rate equations. Numerical results are presented. These results indicate that in a large regime of plasma conditions the LTE assumption is valid for electron temperatures larger than 3000 K.

1. Introduction

The objective of this work is to develop a model to analyze deviations from local thermodynamic equilibrium (LTE) in cesium seeded argon plasmas. Specific evaluations are carried out considering conditions which generally apply to noble gas MHD generators.

In the case of LTE the charged particles concentration $n_e = n_i$ is determined by the Saha equation:

$$n_e^2/n_{Cs} = 2\, g_i/Z^o \,.\, A \,.\, T^{3/2} \,.\, \exp[-(\varepsilon_i - \Delta\varepsilon_i)/kT] \qquad (1)$$

Here, g_i is the degeneracy of the ion ground state (equal to 1 for

Cs^+), $A = (2\pi mk/h^2)^{3/2}$ and $\varepsilon_i/k = 45190$ K is the ionization potential of Cs in temperature units.

$\Delta\varepsilon_i/k$ is the lowering of the ionization potential (see for example [1]):

$$\Delta\varepsilon_i/k = 3.42 \times 10^{-7} \left[n_e(m^{-3})/T(K)\right]^{\frac{1}{2}} \qquad (2)$$

n_{Cs} is the total neutral Cs density (note that the total Cs + Cs^+ density here below is denoted as $n_{Cs} + n_e$). When n_ℓ^o denotes the equilibrium (Boltzmann) population density of the ℓ-th level, n_{Cs} can be written as

$$n_{Cs} = \sum_{\ell=1}^{\ell_{max}} n_\ell^o \qquad (3)$$

Z_o is the partition function of neutral cesium defined by

$$Z^o = \sum_{\ell=1}^{\ell_{max}} g_\ell \exp(-\varepsilon_\ell/kT) \qquad (4)$$

where $\varepsilon_\ell = 0$ for the ground state.

Further we define partial local thermodynamic equilibrium (PLTE) as a situation in which the electrons have a Maxwellian distribution at a temperature T_e and the population densities are equal to b_ℓ times their equilibrium values ($n_\ell = b_\ell n_\ell^o$). The neutral Cs density is then given by

$$n_{Cs} = \sum_{\ell=1}^{\ell_{max}} n_\ell = \sum_{\ell=1}^{max} b_\ell n_\ell^o \qquad (3a)$$

The analogue of the Saha equation becomes

$$n_e^2/n_{Cs} = 2\, g_i/Z \cdot A \cdot T_e^{3/2} \cdot \exp\left[-(\varepsilon_i - \Delta\varepsilon_i)/kT_e\right] \qquad (1a)$$

The PLTE equivalent of Z^o becomes

$$Z = \sum_{\ell=1}^{\ell_{max}} g_\ell b_\ell \exp(-\varepsilon_\ell/kT_e) \qquad (4a)$$

An adequate estimate of Z (or Z^o) for T_e up to 5000 K requires to consider levels up to ε_ℓ = 3.80 eV. For practical purposes it is convenient to average the close-lying levels reducing them to 10 effective levels according to Table 1.

Table 1. Level scheme of Cs

Level	State	Degeneracy, g_ℓ	ε_ℓ, eV
1	6S	2	0
2	6P	6	1.432
3	5D	10	1.805
4	7S	2	2.298
5	7P	6	2.714
6	6D	10	2.804
7	8S+4F	16	3.032
8	8P+7D	36	3.217
9	9S+5F+...+10P	54	3.446
10	Empirical	~ 825	~ 3.68

The last numbers g_{10} and ε_{10} are adjusted to fit the elaborated calculations [1]. In the case of LTE the contribution of the last effective level to Z^o is 6% at 5000 K and less than 2% at 4000 K.

2. Four level model of Cs

When a situation not far from equilibrium is considered (b_ℓ close to unity), usually the approximation can be made that all levels ≥ 2 are in equilibrium with the continuum ($b_\ell \approx 1$) whereas the ground level $\ell = 1$ deviates from equilibrium ($b_1 \neq 1$). Therefore a convenient model should include at least three levels: the ground state, the first excited state and the continuum. To have an estimate of the error introduced by neglecting levels between $\ell = 3$ and $\ell = \ell_{max}$ we also introduce in the balance equations the contribution of the $\ell = 3$ level to $\ell = 1$ and $\ell = 2$ and consider $b_2 \neq 1$. All levels with $\ell \geq 3$ will further be

included in eqs. (3a) and (4a) with values of $b_\ell = 1$ (i.e. all high levels are supposed to be in equilibrium with the continuum). Therefore a four-level model of Cs is considered according to Table 2.

Table 2. Four-level model of Cs

Level	Configuration	Degeneracy	ε_ℓ/k,K	Transition probability, s^{-1}
1	6S	2	0	
2	6P	6	16620	$A_{21} = 3.59 \times 10^7$
3	5D	10	20950	$A_{32} = 0.141 \times 10^7$
4	Continuum	1	45190	

The transition probabilities have been found as averages for $6P_{1/2}$ and $6P_{3/2}$ and correspondingly $5D_{3/2}$ and $5D_{5/2}$ according to (see e.g. Rosado [2])

$$A_{qp} = \sum_i \sum_j g_{q_j} p_i \Big/ \sum g_{q_j} .$$

In this expression A_{ji} is given by

$$A_{ji}(s^{-1}) = 0.667\ \lambda^{-2}\ (cm^{-2})\ f_{ij} g_i/g_j \quad [1]$$

where the oscillator strengths f_{ij} are given in Table 3 [3].

Table 3. Oscillator strengths for Cs transitions

Transition	Oscillator strength
$6S - 6P_{\frac{1}{2}}$	0.394
$6S - 6P_{3/2}$	0.814
$6P_{\frac{1}{2}} - 5D_{3/2}$	0.251
$6P_{3/2} - 5D_{3/2}$	0.0211
$6P_{3/2} - 5D_{5/2}$	0.204

3. Balance equations

Following Rosado's notation [2] we write the balance equations for the ground state and the first excited level under the assumption of a Maxwellian distribution of electrons:

$$n_e(K_{12} + K_{13} + K_{1i})\delta b_1 - (n_e K_{12} + R_{21}A_{21}\Lambda_{21})\delta b_2 =$$

$$R_{1i}^{(2)}K_{i1}^{(2)}\Lambda_{i1}^{(2)} + R_{21}A_{21}\Lambda_{21} + \text{Dif.} \qquad (5a)$$

$$-n_e K_{21}\delta b_1 + [n_e(K_{21} + K_{23} + K_{2i}) + A_{21}\Lambda_{21}]\delta b_2 =$$

$$R_{2i}^{(2)}K_{i2}^{(2)}\Lambda_{i2}^{(2)} - A_{21}\Lambda_{21} + R_{32}A_{32}\Lambda_{32} \qquad (5b)$$

where

$$\delta b_q = b_q - 1,$$

$$R_{rq} = n_r^o/n_q^o = (g_r/g_q)\exp\left[-(\varepsilon_r - \varepsilon_q)/kT_e\right] = K_{qr}/K_{rq}, \text{ and}$$

$$R_{qi}^{(2)} = n_e^2/n_q^0 = (2\, g_i/g_q)\, AT_e^{3/2} \exp\left[-(\varepsilon_i - \Delta\varepsilon_i - \varepsilon_q)/kT_e\right].$$

K_{rq} are the electron excitation (de-excitation) rates $r \to q$. K_{ri} are the ionization rates $r \to i$; $K_{ir}^{(2)}$ are the radiative recombination rate coefficients and Λ (indexed corresponding to the transition considered) represents the escape factor for line or continuum radiation. Note that the indices ℓ, r, q stand for atomic levels while i stands for the Cs ion.

If eq. (5b) is multiplied by R_{21}, added to eq. (5a) while dropping terms including index 3, then a balance equation for Cs^+ will follow. In eq. (5a) the loss of ground state particles (the first term of the L.H.S.) is compensated by what is coming from the excited level, from the continuum and from the inward flow of ground level atoms. For steady state conditions this flow is equal to the outward flow of ions (provided that $n_2 << n_1$). The inward flow of ground level atoms is

represented by Dif > 0 defined by

$$Dif = \text{div}\,(n_e \underline{W}_A)/n_1^o$$

In this expression $n_e \underline{W}_A = -n_1 \underline{W}_1$ where $\underline{W}_A$ is the ambipolar diffusion velocity. Eq. (5b) represents the balance of the 6P level and is built the same way, but also the 5D level (index 3) is taken into account and the diffusion of the 6P level particles is neglected because $n_2 << n_1$.

4. Collisional rate coefficients

The electronic excitation rate coefficients K_{rq} (and analogous the ionization rate coefficients K_{ri}) are given by [4]:

$$K_{rq} = \left(\frac{8\ kT_e}{\pi m}\right)^{\frac{1}{2}} \int_{\varepsilon_{rq}/kT_e}^{\infty} x e^{-x}\, Q_{rq}(\varepsilon)dx, \qquad (6)$$

Q_{rq} being the cross section of the proces r → q and x being given by $x = \varepsilon/kT_e$. For $kT_e < \varepsilon_{rq}$ Q_{rq} can be approximated by

$$\begin{aligned} Q_{rq} &= a(\varepsilon - \varepsilon_{rq}) \quad \text{for} \quad \varepsilon_{rq} < \varepsilon < \varepsilon^* \\ Q_{rq} &= a(\varepsilon^* - \varepsilon_{rq}) + a^*(\varepsilon - \varepsilon^*) \quad \text{for} \quad \varepsilon^* < \varepsilon \end{aligned} \qquad (7)$$

Then eq. (6) becomes

$$K_{rq} = B\big[a(\varepsilon_{rq}/kT_e + 2)\ \exp\ (-\varepsilon_{rq}/kT_e) -$$

$$(a - a^*)\ (\varepsilon^*/kT_e + 2)\ \exp\ (-\varepsilon^*/kT_e)\big] \qquad (8)$$

with $B = (8\ kT_e/\pi m)^{\frac{1}{2}}\ kT_e = 8.58 \times 10^{-20}\ T_e^{3/2}$ J m/s.

According to the formula of Drawin (see for example [4]) $a \sim \varepsilon_{rq}^{-3}$. Then in a rough approximation $K_{rq} \sim \exp\ (-\varepsilon_{rq}/kT_e)/\varepsilon_{rq}^2$. Therefore, in the eqs. (5) $K_{13} << K_{12}$; $K_{1i} << K_{12}$ and $K_{2i} << K_{23}$. The remaining electron-

ic excitation rate coefficients may be calculated according to Table 4.

Table 4. Collisional excitation cross-section characteristics

Transition	a, m^2/J	a*, m^2/J	ε_{rq}/k, K	ε^*/k, K	Reference
1 - 2	6.45	0.75	16620	23440	[5]
2 - 3	75	0	4330	7580	

The figures in the last line of Table 4 are based on an approximation using the Drawin formula (see for example [4] with $\beta_1 = 1$ and $\beta_2 = 1.6$. The de-excitation rate (2 - 1) is taken as $K_{21} = K_{12} \exp(-\varepsilon_{12}/kT_e)/3$ in accordance with detailed balancing.

5. Radiative rate coefficients and escape factors

The radiative two-body recombination rate coefficients are given by

$$K_{iq}^{(2)} = (8\ kT_e/\pi m)^{\frac{1}{2}} \int_0^\infty x e^{-x} Q_{iq} dx \qquad (9a)$$

For small electron energies Q_{iq} is proportional to ε^{-1}, $Q_{iq} = mC_{iq}/2\varepsilon$:

$$K_{iq}^{(2)} = 2(m/2\pi kT_e)^{\frac{1}{2}} C_{iq} \qquad (9b)$$

For q = 1,2 $C_{iq} = 1.77 \times 10^{-16}$ m^4/s and 2.79×10^{-14} m^4/s correspondingly (see for example [6]).
Now using the expression $R_{qi}^{(2)}$ given in section 3 we come to

$$K_{iq}^{(2)} R_{qi}^{(2)} = (8\ m/\pi k)^{\frac{1}{2}} (C_{iq} T_e/g_q)\ A \exp\left[-(\varepsilon_i - \varepsilon_q)/kT_e\right] =$$

$$= 0.99 \times 10^{18} (C_{iq} T_e/g_q) \exp\left[-(45190 - \Delta\varepsilon_i/k - \varepsilon_q/k)/T_e\right] \qquad (10)$$

The evaluations show that in the cases of practical interest (arcs and MHD conversion) the terms $R^{(2)}_{qi} K^{(2)}_{iq} \Lambda^{(2)}_{iq}$ ($\Lambda^{(2)}_{iq} \simeq 1$) in the right sides of equations (5) may be neglected. Note that if we consider the balance equation for Cs^+ these terms will be important.

The escape factor for a bound-bound transition is given by

$$\Lambda_{rq} = \alpha/(\pi k_{qr} r)^{\frac{1}{2}} \tag{11a}$$

(see for example [4], where $\alpha = 1.115$ for a cylindrically symmetric plasma with a radius r. The absorption in a center of a line is

$$k_{qr} = e^2 f_{qr} n_q / 2\pi\varepsilon_o mc\Delta\nu \tag{11b}$$

and the half half-width $\Delta\nu$ consists of two parts [7]: Van der Waals broadening due to collisions with Ar

$$\Delta\nu_w = 2.71(C_6/h)^{0.4}\{8\ kT_g(m_{Ar}^{-1} + m_{Cs}^{-1})/\pi\}^{0.3} n_{Ar} \tag{11c}$$

(Tg is the temperature of the heavy particles) and resonant broadening

$$\Delta\nu_R = (3e^2/16\pi^2\varepsilon_o mc)\ (g_q/g_r)^{\frac{1}{2}} \lambda_{rq} f_{qr} n_q \tag{11d}$$

(λ_{rq} is the transition wavelength). The Van der Waals constant is $C_6 = \frac{1}{3} C_6(Cs6P_{1/2} - Ar_{1/2,\ 1/2}) + \frac{2}{3}[\frac{1}{3} C_6(Cs6P_{3/2} - Ar_{3/2,\ 1/2}) + \frac{2}{3} C_6(Cs6P_{3/2} - Ar_{3/2,\ 3/2})] = 6.11 \times 10^{-77}$ Jm^6 for the first excited level of Cs, the values of C_6 corresponding to the different transitions being according to [8] 6.13, 7.90 and 5.19×10^{-77} Jm^6 in the order of their appearance in the above formula.

Finally for the transition 6P - 6S we come to

$$\Lambda_{21} = 9.23 \times 10^{-6}\ T_g^{0.15}\ [(n_{Cs} + n_e)/n_1 sr]^{\frac{1}{2}} x$$

$$(1 + 277\ n_1 s/n_{Cs} T_g^{0.3})^{\frac{1}{2}} \tag{12}$$

where s is the seed fraction, $s = (n_{Cs} + n_e)/n_{Ar}$,

$$\frac{n_{Cs} + n_e}{n_1} = \frac{1}{2\, b_1} \{Z + 2g_i AT^{3/2} \exp [-(\varepsilon_i - \Delta\varepsilon_i)/kT_e]/n_e\},\ T_g \text{ is in K}$$

and r in m.

The second term in the last parentheses in eq. (12) is equal to the ratio $\Delta\nu_R/\Delta\nu_w$. Under the conditions of close-cycle MHD conversion it is small (~ 0.1) so that the resonant broadening is not important and therefore the last factor in eq. (12) may be omitted.

Now let us consider the escape factor for the transition 3-2. In this case $\Delta\nu_R$ is much smaller than $\Delta\nu_w$ (compare eqs. (11d) and (11c)) and therefore should be neglected. The Van der Waals broadening may be estimated by a comparison with the transition 2-1:

$$\frac{\Delta\nu_w(3\text{-}2)}{\Delta\nu_w(2\text{-}1)} = \left[\frac{\varepsilon_2(\varepsilon_i - \varepsilon_2)}{\varepsilon_3(\varepsilon_i - \varepsilon_3)}\right]^{0.8}$$

(see for example [9]). Then

$$\frac{\Lambda_{32}}{\Lambda_{21}} = \left(\frac{f_{12}}{f_{23}}\right)^{\frac{1}{2}} \left(\frac{h_1}{h_2}\right)^{\frac{1}{2}} \left[\frac{\varepsilon_2(\varepsilon_i - \varepsilon_2)}{\varepsilon_3(\varepsilon_i - \varepsilon_3}\right]^{0.4},$$

$f_{12} = 0.674$, $f_{23} = 0.2$ (values averaged over sublevels) and

$$\Lambda_{32} = 10.5 \times 10^{-6}\, T_g^{0.15} \left[(n_{Cs} + n_e)/n_2 sr\right]^{\frac{1}{2}} \qquad (13)$$

6. Diffusion

As was mentioned in section 3 the diffusion term in eq. (5a) is $\mathrm{Dif} = \mathrm{div}\,(n_e \underline{W}_a)/n_1^o$. The diffusion flux density is

$$n_e \underline{W}_a = -(D_A/2kT_i)\nabla(p_e + p_i) \qquad (14a)$$

where $D_A = 2\, D_{ia}$ is the ambipolar diffusion coefficient.

The equation (14a) is easily transformed into

$$n_e \underline{W}_a = -(n_e D_A/2)\left[(1 + T_e/T_i)\nabla \ln n_e + \nabla \ln T_i + (T_e/T_i)\nabla \ln T_e\right] \qquad (14b)$$

The radial dependences of n_e, T_e, T_i may be approximated by

$$n_e = n_{eo} \exp\left[-(\rho/\rho_o)^2\right] \qquad (15a)$$

$$T_e = T_{eo} \exp\left[-(\rho/2.3\rho_o)^2\right] \qquad (15b)$$

$$T_i = T_{i\infty} + (T_{io} - T_{i\infty}) \exp\left[-(\rho/\rho o)^2\right], \qquad (15c)$$

where n_{eo}, T_{eo} and T_{io} are values at the axis, $T_{i\infty}$ is the ion temperature outside the arc and ρ_o is the equivalent radius of the arc, $\rho_o = r$ in the notation of section 5. We found that equations (15) fit well the experimental data of [2] and [9] for a wide range of current densities (10^4 to 3×10^6 A/m^2).

Now we use eq. (14b) and eqs. (15) to find out the diffusion term:

$$\mathrm{Dif} = \frac{1}{n_1^o} \cdot \frac{1}{\rho} \frac{d}{d\rho} (\rho n_e W_A) =$$

$$= \frac{2D_A n_e}{n_1^o \rho_o^2} \left(2.19 + \frac{T_e}{T_i} - \frac{T_{i\infty}}{T_i}\right)\left[1 - \left(\frac{\rho}{\rho_o}\right)^2 f\left(\frac{\rho}{\rho_o}\right)\right] \qquad (16)$$

The function $f(\frac{\rho}{\rho_o})$ is monotonic and equal to 1.5 at $\rho = 0$ and to 1.1 at $\rho \to \infty$. For further estimations the last factor in eq. (16) will be taken at $(\rho/\rho_o) = 0.25$: $f(\rho/\rho_o) \simeq 0.9$.

Typical values for a closed-cycle MHD generator are: $T_e/T_i \simeq 3$; $T_{i\infty}/T_i \simeq 0.75$; taking into account the relation $R_{1i}^{(2)} = n_e^2/n_1^o$ from section 3 we come to

$$\mathrm{Dif} = 8D_A R_{1i}^{(2)}/n_e \rho_o^2 \qquad (17)$$

The coefficient of diffusion of ions through neutrals D_{ia} is determined mostly by interactions Cs^+-Ar. Data for the mobility μ of Cs^+ through Ar are available [10]: at normal density ($N_o = 2.69 \times 10^{25}\ m^{-3}$) $\mu_o = 2.07\ cm^2/Vs$. To calculate D_{ia} we use the Einstein relation $D = kT_g\mu/e$; taking into account the proportionality $\mu \sim N_o/n_{Ar}$ we come to

$$D_{ia} = \frac{(kT_g)^2}{e}\,\mu_o\,\frac{N_o}{p}$$

and therefore

$$D_A = 2\,D_{ia} = 1.33 \times 10^{-10}\,T_g^2(K^2)/p(Bar)\ m^2/s \qquad (18)$$

In obtaining eq. (18) we assumed that the product μn_{Ar} does not depend on T_g which agrees well with the experimental data. On the other hand it is well known [11] that $pD \sim T^{3/2}/\Omega^*$, where Ω^* is the dimensionless collision integral. For a purely attractive or repulsive interaction with a potential energy $\sim R^{-\delta}$ (R is the distance between the particles) $\Omega^* \sim T^{-2/\delta}$. As the potential well depth ε/k of the Cs^+-Ar interaction is of the order of *1000 K the attraction prevails; for a pair ion +* neutral $\delta = 4$. Therefore $\Omega^* \sim T^{-1/2}$ and $pD \sim T^2$ in accordance with eq. (18).

7. Solution of the balance equations

With small terms neglected the system of equations (5) becomes

$$\delta b_1 - (1 + R_{21}A_{21}\Lambda_{21}/n_eK_{12})\delta b_2 =$$

$$(R_{21}A_{21}\Lambda_{21} + Dif)/n_eK_{12} \qquad (19a)$$

$$\delta b_1 - (1 + K_{23}/K_{21} + A_{21}\Lambda_{21}/n_eK_{21})\delta b_2 =$$

$$(A_{21}\Lambda_{21} - R_{32}A_{32}\Lambda_{32})/n_eK_{21} \qquad (19b)$$

The numerical results discussed in the next section are obtained by

solving this system of equations.

Simplified expression for δb_1 and n_e/n_e^o can be obtained in the following way. We may assume $\delta b_2 << \delta b_1$ and $\delta b_1 < 1$. Let us denote $R_{21}A_{21}\Lambda_{21}/n_e K_{12} \equiv Q_R$ and $Dif/n_e K_{12} \equiv Q_D$; then $\delta b_1 = Q_R + Q_D$. If the seed fraction and the pressure are not very low, then a substantial deviation from LTE takes place only at low temperatures ($T_e < 3000$ K), where $(n_{Cs} + n_e)/n_1 \simeq 1$ (moderate degree of ionization). Using eq. (8) for K_{12} (without the second term in the brackets which represents a small correction), eq. (12) for Λ_{21} and eqs. (17) and (18) for the diffusion term we estimate the relative contribution of the diffusion to be

$$\frac{Q_D}{Q_R} = \frac{2.58 \times 10^{-11}\, T_g^{1.85} T_e^{1.5} s^{0.5}}{\exp(28500/T_e)\, pr^{1.5} (n_e/10^{20})} \qquad (20)$$

(T is in K, p is in Bar, r is in m and n_e is in m^{-3}). For $Q_D/Q_R > 1$ the deviation from LTE is dominated by the diffusion. For a radiation escape regime $Q_D/Q_R < 1$ and

$$\delta b_1 = 1.08 \times 10^{-3} \frac{T_g^{0.15}}{(T_e sr)^{0.5} (n_e/10^{20})} \qquad (21)$$

(if $\delta b_2 << \delta b_1$, $\delta b_1 < 1$) and $(n_{Cs} + n_e)/n_1 < 1$).

Note that the overpopulation of the ground state corresponds (for moderate degrees of ionization) to a decrease in the ion density,

$$n_e \simeq n_e^o (1 + \delta b_1)^{-\frac{1}{2}} \qquad (22)$$

Eq. (22) follows from eqs. (1), (4), (1a) and (4a) provided $n_1 \simeq n_{Cs}$. It is consistent with the result of Mitchner and Kruger [4] (their equation 3.6 of Ch. IX).

8. Results and discussions

Numerical results obtained by the solution of eqs. (19a) and (19b) are

represented by Figs. 1 - 16. The results refer to cylindrical discharges with radial distribution of n_e, T_e and T_i according to eqs. 15a, 15b and 15c. The figures show δb_1, δb_2, n_e and n_e/n_e^o as functions of the electron temperature. Parametric variation has been applied involving the radius, the gas temperature, the pressure and the seed fraction according to Table 5.

Table 5. Parametric variations.

Curve	radius	gas temperature	pressure	seed fraction
a	0.1 mm	$T_e/2$	0.1 bar	0.2×10^{-3}
b	0.316 mm	$T_e/3$	0.316 bar	1.0×10^{-3}
c	1.0 mm	$T_e/4$	1.0 bar	5.0×10^{-3}

The general feature of all the figures is that strong deviations from LTE occur at electron temperatures lower than 3000 K. This is caused by the fact that at such low electron temperatures the electron density becomes so small that the electron collisions can no longer dominate the diffusion and radiation processes. The other parameters change the electron temperature below which deviation from LTE occurs, but for the given parameter variation this change is not dramatical.

Figs. 1 - 4 show the influence of the radius of the discharge. A smaller radius results in a larger deviation from LTE because of a larger diffusion and a smaller absorption of radiation. The increase of δb_1 and δb_2 at high electron temperatures occurs when the neutral cesium concentration considerably decreases due to ionization. The electron density keeps approaching the equilibrium value with increasing electron temperature (Fig. 4). The decrease of the electron density between T_e = 4000 K and T_e = 5000 K is caused by the determination of the value of the gas temperature. Because the gas temperature is determined as a fraction of the electron temperature it increases with T_e.
Since the pressure is a fixed number the total cesium density (neutrals plus ions) decreases with T_e causing a decrease of n_e^o when its value is close to complete ionization.

Figs. 5 - 8 exhibit the effect of variation in gas temperature. Larger gas temperatures correspond to larger deviations from LTE which are caused by larger escape factors (eqs. 12, 13) and larger diffusion coefficients (eq. 18). The large differences in the maximum values of n_e (Fig. 7) result from the different values of $n_{Cs} + n_e$ for the three cases considered following from the three different temperatures all taken at the same pressure.

Figs. 9 - 12 demonstrate how the pressure affects LTE. Lower pressures cause a larger deviation than higher pressures due to a larger diffusion. The differences in the curves for n_e (Fig. 11) are again the result of different values of $n_{Cs} + n_e$.

Figs. 13 - 16 represent changes of the nonequilibrium situation due to variations in seed fraction. From the parametric variations considered the seed fraction variation affects the deviation from LTE the most (compare Figs. 1, 5, 9 and 13). A low seed fraction increases the escape of radiation according to eqs. 12 and 13. Furthermore a lower seed fraction results in a lower electron density and therefore in lower collisional (de)excitation rates. Fig. 15 exhibits again the different values of $n_{Cs} + n_e$ for each curve.

9. Conclusions

The assumption of local thermodynamic equilibrium has been analyzed for *stationary discharges in cesium seeded argon plasmas*. The following conditions have been considered:

- $2000\ K < T_e < 5000\ K$
- $T_e/2 < T_g < T_e/4$
- 0.1 mm < radius < 1.0 mm
- 0.1 bar < p < 1.0 bar
- $0.2 \times 10^{-4} <$ seed fraction $< 5.0 \times 10^{-4}$

For these conditions a noticable deviation of n_e from its LTE value is only found when $T_e < 3000$ K. Deviations of n_1 and n_2 from their equilibrium values occur also at higher electron temperatures at large degrees of ionization.

The deviation from LTE is amplified by the following changes of parameters:

- increase of gas temperature.
- decrease of radius.
- decrease of pressure.
- decrease of seed fraction.

Acknowledgement

This work has been carried out as a part of the research program of the Shock tube MHD Project of the Group Direct Energy Conversion at the Eindhoven University of Technology.
The investigations have been accomplished during a visit of the first and second author to the Eindhoven University of Technology. This visit has been financially supported by the Dutch Organization for Pure Scientific Research (Z.W.O.).

References

[1] Drawin, H.W. and P. Felenbok
DATA FOR PLASMAS IN LOCAL THERMODYNAMIC EQUILIBRIUM.
Paris: Gauthier-Villars, 1965.

[2] Rosado, R.J.
AN INVESTIGATION OF NON-EQUILIBRIUM EFFECTS IN THERMAL ARGON PLASMAS.
Ph.D. Thesis. Eindhoven University of Technology, 1981.

[3] Smirnov, B.M.
ATOMIC COLLISIONS AND ELEMENTARY PROCESSES IN A PLASMA (in Russian).
Moscow: Atomizdat, 1968.

[4] Mitchner, M. and Ch.H. Kruger, Jr.
PARTIALLY IONIZED GASES.
New York: Wiley, 1973.
Wiley series in plasma physics

[5] Chen, S.T. and A.C. Gallagher
ELECTRON EXCITATION OF THE RESONANCE LINES OF THE ALKALI-METAL ATOMS.
Phys. Rev. A, Vol. 17(1978), p. 551-560.

[6] Borghi, C.A.
DISCHARGES IN THE INLET REGION OF A NOBLE GAS MHD GENERATOR.
Ph.D. Thesis. Eindhoven University of Technology, 1982.

[7] Hindmarsh, W.R. and J.M. Farr
COLLISION BROADENING OF SPECTRAL LINES BY NEUTRAL ATOMS.
Prog. Quantum Electron., Vol. 2(1972), p. 141-214.

[8] Mahan, J.D.
VAN DER WAALS CONSTANT BETWEEN ALKALI AND NOBLE-GAS ATOMS. II. Alkali atoms in excited states.
J. Chem. Phys., Vol. 50(1969), p. 2755-2758.

[9] Wetzer, J.M.
SPATIALLY RESOLVED DETERMINATION OF PLASMA PARAMETERS OF A NOBLE GAS LINEAR MHD GENERATOR.
Ph.D. Thesis. Eindhoven University of Technology, 1984.

[10] Hasted, J.B.
PHYSICS OF ATOMIC COLLISIONS.
London: Butterworth, 1964.
Butterworths advanced physics series

[11] Hirschfelder, J.O. and Ch.F. Curtiss, R.B. Bird
MOLECULAR THEORY OF GASES AND LIQUIDS.
New York: Wiley, 1954. 4th printing 1967.
Structure of matter series
P. 527.

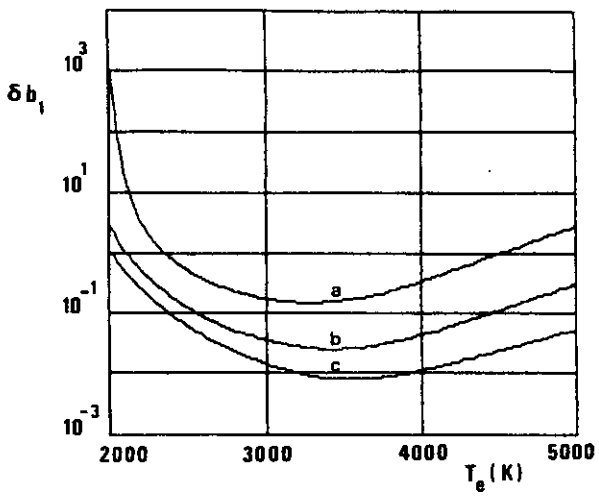

Fig. 1. Relative overpopulation of the ground state (δb_1) as a function of electron temperature (T_e).
p=0.316 bar; $T_g=T_e/3$; seed fraction=$1x10^{-3}$.
a. r=0.1 mm; b. r=0.316 mm; c. r=1.0 mm.

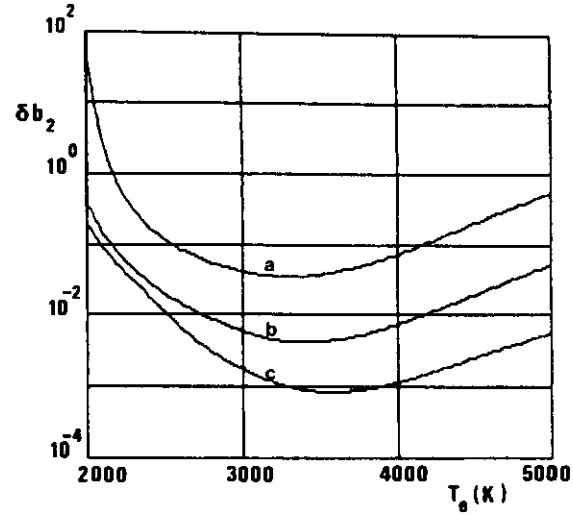

Fig. 2. Relative overpopulation of the first excited state (δb_2) as a function of electron temperature (T_e).
p=0.316 bar; $T_g=T_e/3$; seed fraction=$1x10^{-3}$.
a. r=0.1 mm; b. r=0.316 mm; c. r=1.0 mm.

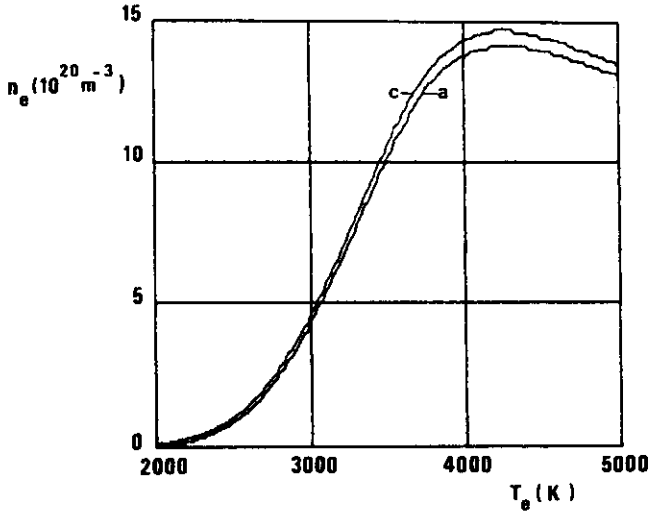

Fig. 3. Electron density (n_e) as a function of electron temperature (T_e).
p=0.316 bar; $T_g=T_e/3$; seed fraction=$1x10^{-3}$.
a. r=0.1 mm; c. r=1.0 mm.

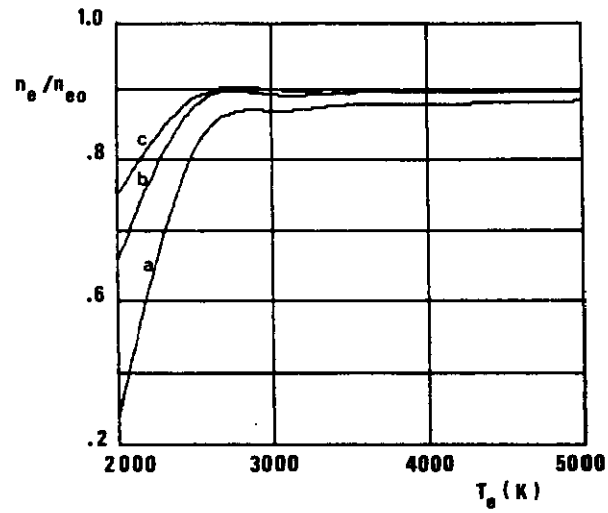

Fig. 4. Ratio of electron density to its equilibrium value (n_e/n_e^o) as a function of electron temperature (T_e).
p=0.316 bar; $T_g=T_e/3$; seed fraction=$1x10^{-3}$.
a. r=0.1 mm; b. r=0.316 mm; c. r=1.0 mm.

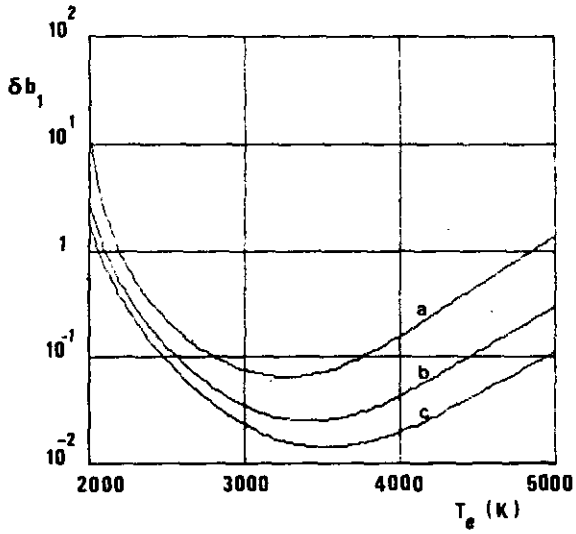

Fig. 5. Relative overpopulation of the ground state (δb_1) as a function of electron temperature (T_e).
p=0.316 bar; seed fraction=1x10^{-3}; r=0.316 mm.
a. $T_g=T_e/2$; b. $T_g=T_e/3$; c. $T_g=T_e/4$.

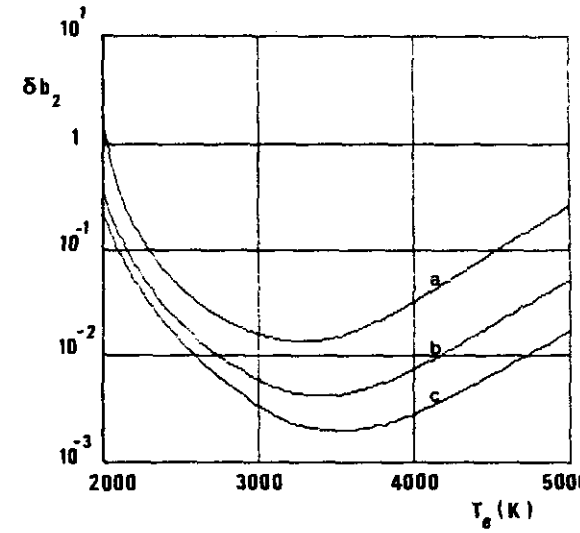

Fig. 6. Relative overpopulation of the first excited state (δb_2) as a function of electron temperature (T_e).
p=0.316 bar; seed fraction=1x10^{-3}; r=0.316 mm.
a. $T_g=T_e/2$; b. $T_g=T_e/3$; c. $T_g=T_e/4$.

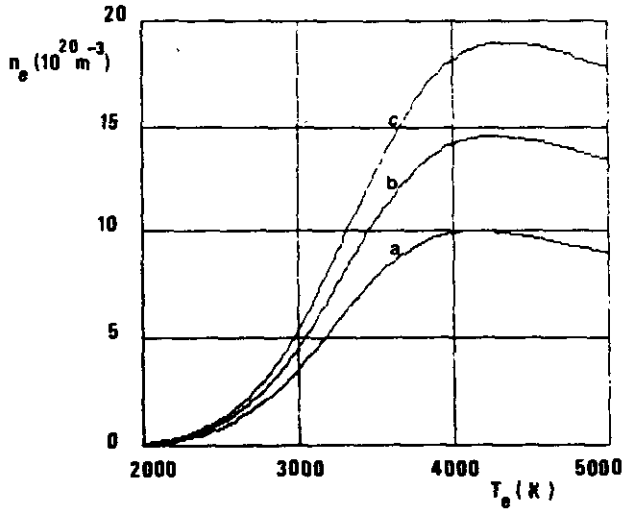

Fig. 7. Electron density (n_e) as a function of electron temperature (T_e).
p=0.316 bar; seed fraction=1x10^{-3}; r=0.316 mm.
a. $T_g=T_e/2$; b. $T_g=T_e/3$; c. $T_g=T_e/4$.

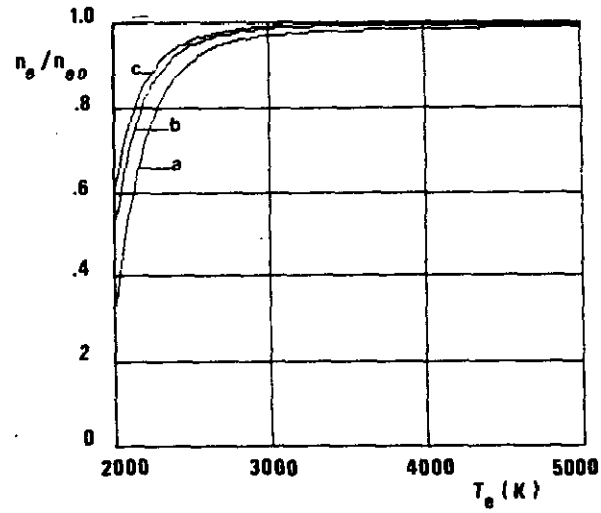

Fig. 8. Ratio of the electron density to its equilibrium value (n_e/n_e^o) as a function of electron temperature (T_e).
p=0.316 bar; seed fraction=1x10^{-3}; r=0.316 mm.
a. $T_g=T_e/2$; b. $T_g=T_e/3$; c. $T_g=T_e/4$.

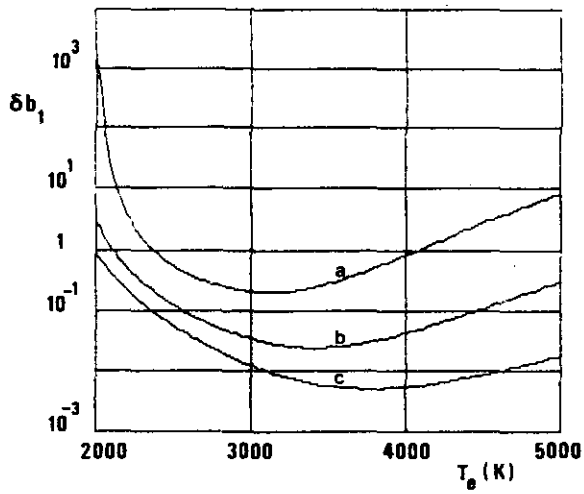

Fig. 9. Relative overpopulation of the ground state (δb_1) as a function of electron temperature (T_e).
$T_g = T_e/3$; seed fraction=1×10^{-3}; r=0.316 mm.
a. p=0.1 bar; b. p=0.316 bar; c. p=1 bar.

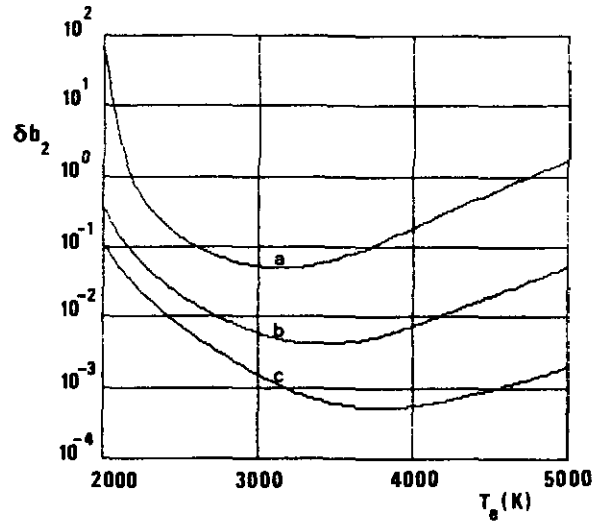

Fig. 10. Relative overpopulation of the first excited state (δb_2) as a function of electron temperature (T_e).
$T_g = T_e/3$; seed fraction=1×10^{-3}; r=0.316 mm.
a. p=0.1 bar; b. p=0.316 bar; c. p=1 bar.

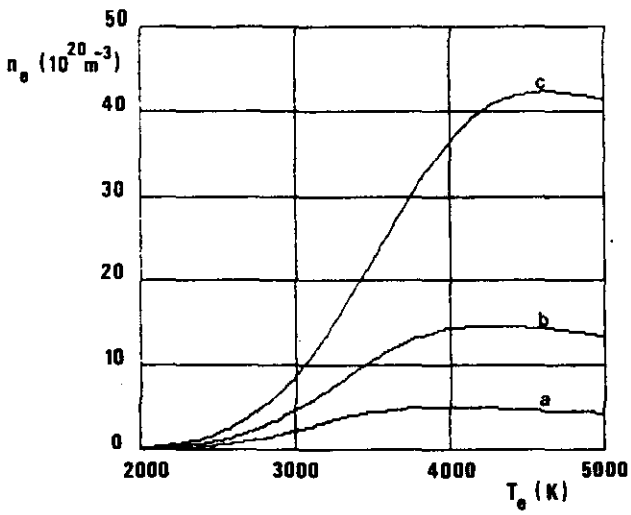

Fig. 11. Electron density (n_e) as a function of electron temperature (T_e).
$T_g = T_e/3$; seed fraction=1×10^{-3}; r=0.316 mm.
a. p=0.1 bar; b. p=0.316 bar; c. p=1 bar.

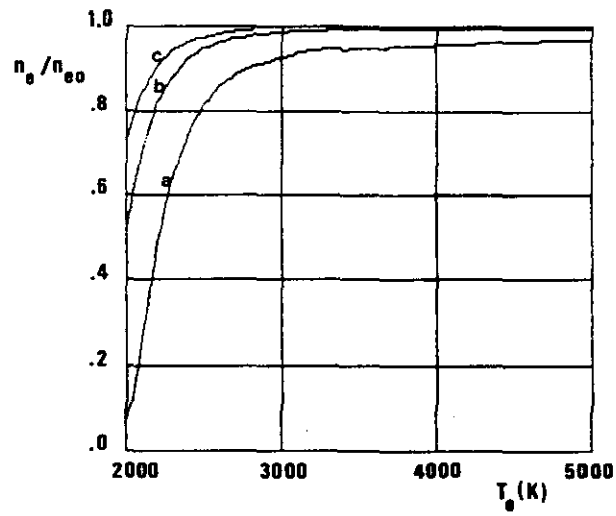

Fig. 12. Ratio of the electron density to its equilibrium value (n_e/n_e^o) as a function of electron temperature (T_e).
$T_g = T_e/3$; seed fraction=1×10^{-3}; r=0.316 mm.
a. p=0.1 bar; b. p=0.316 bar; c. p=1 bar.

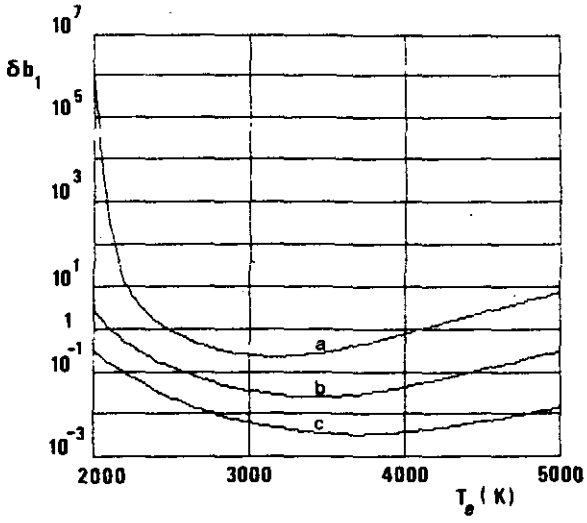

Fig. 13. Relative overpopulation of the ground state (δb_1) as a function of electron temperature (T_e).
p=0.316 bar; r=0.316 mm; $T_g=T_e/3$.
a. seed fraction=0.2×10^{-3};
b. seed fraction=1.0×10^{-3};
c. seed fraction=5.0×10^{-3}.

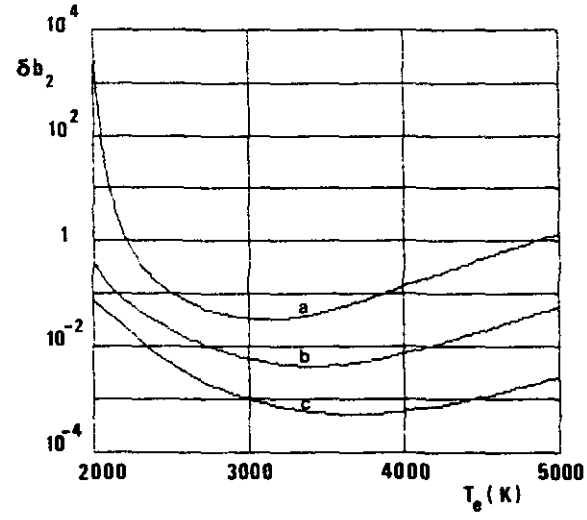

Fig. 14. Relative overpopulation of the first excited state (δb_2) as a function of electron temperature (T_e).
p=0.316 bar; r=0.316 mm; $T_g=T_e/3$.
a. seed fraction=0.2×10^{-3};
b. seed fraction=1.0×10^{-3};
c. seed fraction=5.0×10^{-3}.

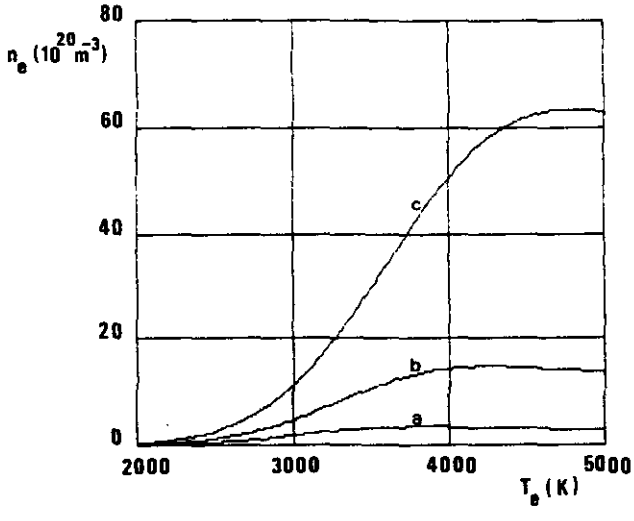

Fig. 15. Electron density (n_e) as a function of electron temperature (T_e).
p=0.316 bar; r=0.316 mm; $T_g=T_e/3$.
a. seed fraction=0.2×10^{-3};
b. seed fraction=1.0×10^{-3};
c. seed fraction=5.0×10^{-3}.

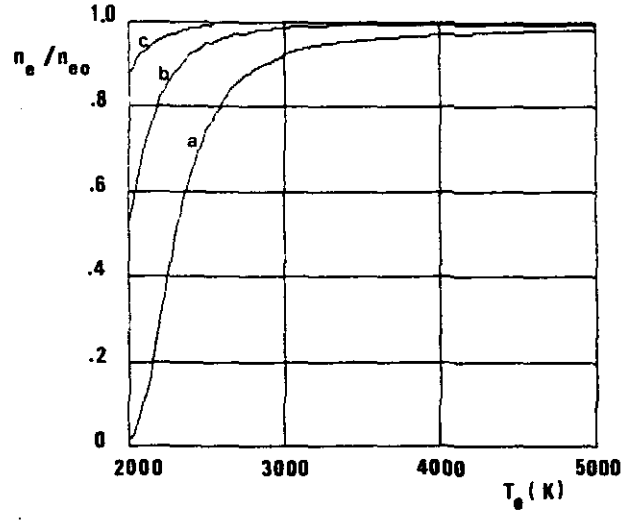

Fig. 16. Ratio of the electron density to its equilibrium value (n_e/n_e^o) as a function of electron temperature (T_e).
p=0.316 bar; r=0.316 mm; $T_g=T_e/3$.
a. seed fraction=0.2×10^{-3};
b. seed fraction=1.0×10^{-3};
c. seed fraction=5.0×10^{-3}.

EINDHOVEN UNIVERSITY OF TECHNOLOGY
THE NETHERLANDS
DEPARTMENT OF ELECTRICAL ENGINEERING

Coden: TEUEDE

Eindhoven University of Technology Research Reports (ISSN 0167-9708):

(138) Nicola, V.F.
A SINGLE SERVER QUEUE WITH MIXED TYPES OF INTERRUPTIONS: Application to the modelling of checkpointing and recovery in a transactional system.
EUT Report 83-E-138. 1983. ISBN 90-6144-138-2

(139) Arts, J.G.A. and W.F.H. Merck
TWO-DIMENSIONAL MHD BOUNDARY LAYERS IN ARGON-CESIUM PLASMAS.
EUT Report 83-E-139. 1983. ISBN 90-6144-139-0

(140) Willems, F.M.J.
COMPUTATION OF THE WYNER-ZIV RATE-DISTORTION FUNCTION.
EUT Report 83-E-140. 1983. ISBN 90-6144-140-4

(141) Heuvel, W.M.C. van den and J.E. Daalder, M.J.M. Boone, L.A.H. Wilmes
INTERRUPTION OF A DRY-TYPE TRANSFORMER IN NO-LOAD BY A VACUUM CIRCUIT-BREAKER.
EUT Report 83-E-141. 1983. ISBN 90-6144-141-2

(142) Fronczak, J.
DATA COMMUNICATIONS IN THE MOBILE RADIO CHANNEL.
EUT Report 83-E-142. 1983. ISBN 90-6144-142-0

(143) Stevens, M.P.J. en M.P.M. van Loon
EEN MULTIFUNCTIONELE I/O-BOUWSTEEN.
EUT Report 84-E-143. 1984. ISBN 90-6144-143-9

(144) Dijk, J. and A.P. Verlijsdonk, J.C. Arnbak
DIGITAL TRANSMISSION EXPERIMENTS WITH THE ORBITAL TEST SATELLITE.
EUT Report 84-E-144. 1984. ISBN 90-6144-144-7

(145) Weert, M.J.M. van
MINIMALISATIE VAN PROGRAMMABLE LOGIC ARRAYS.
EUT Report 84-E-145. 1984. ISBN 90-6144-145-5

(146) Jochems, J.C. en P.M.C.M. van den Eijnden
TOESTAND-TOEWIJZING IN SEQUENTIELE CIRCUITS.
EUT Report 85-E-146. 1985. ISBN 90-6144-146-3

(147) Rozendaal, L.T. en M.P.J. Stevens, P.M.C.M. van den Eijnden
DE REALISATIE VAN EEN MULTIFUNCTIONELE I/O-CONTROLLER MET BEHULP VAN EEN GATE-ARRAY.
EUT Report 85-E-147. 1985. ISBN 90-6144-147-1

(148) Eijnden, P.M.C.M.
A COURSE ON FIELD PROGRAMMABLE LOGIC.
EUT Report 85-E-148. 1985. ISBN 90-6144-148-X

(149) Beeckman, P.A.
MILLIMETER-WAVE ANTENNA MEASUREMENTS WITH THE HP8510 NETWORK ANALYZER.
EUT Report 85-E-149. 1985. ISBN 90-6144-149-8

EINDHOVEN UNIVERSITY OF TECHNOLOGY
THE NETHERLANDS
DEPARTMENT OF ELECTRICAL ENGINEERING

Coden: TEUEDE

Eindhoven University of Technology Research Reports (ISSN 0167-9708):

(150) Meer, A.C.P. van
EXAMENRESULTATEN IN CONTEXT MBA.
EUT Report 85-E-150. 1985. ISBN 90-6144-150-1

(151) Ramakrishnan, S. and W.M.C. van den Heuvel
SHORT-CIRCUIT CURRENT INTERRUPTION IN A LOW-VOLTAGE FUSE WITH ABLATING WALLS.
EUT Report 85-E-151. 1985. ISBN 90-6144-151-X